Data-Driven Gas Sensing Analysis of Titanium-Doped Cadmium Oxide Thin Films

Muna Ahmed Issa[1], Nazar Abdulmahdi Jabir[2], Athraa Naji Jameel[3], Muhaned Zaidi[4] and Hassan Hadi Darwoysh[3]

[1]*Quality Assurance and Performance Evaluation Department, Mustansiriyah University, 10052 Baghdad, Iraq*
[2]*Department of Physics, College of Science, Mustansiriyah University, 10052 Baghdad, Iraq*
[3]*Department of Physics, College of Education, Mustansiriyah University, 10052 Baghdad, Iraq*
[4]*Department of Medical Physics, College of Science, Al-Manara University, 62001 Amarah, Iraq*
muna.ahmed@uomustansiriyah.edu.iq, nazar.j@uomustansiriyah.edu.iq, athraanaje@uomustansiriyah.edu.iq, muhanedzaidi@uomanara.edu.iq, hassan.hadi66@uomustansiriyah.edu.iq

Keywords: Tio2 Thin Films, Plasma Jet, XRD, AFM, Band Gap, Resistance, Sensitivity.

Abstract: TiO_2: Sn thin films were prepared using the plasma jet technique at different discharge voltages (12, 13, and 14 kV). X-ray diffraction analysis exhibited that all samples were cubic polycrystalline with a dominant peak at the (101) plane. The grain size was expanded from 16.93 nm to 19.39 nm by increasing the discharge voltage. However, it caused a decrease in dislocation density (δ) values from 34.82 to 26.59. In addition, strain (ε) is decreased from 20.47 to 17.88. The AFM images showed an average grain size of approximately 81.79 –52.64nm, and the root mean square roughness (Rrms) decreased from 3.31 nm to 5.98 nm when the discharge voltage was increased to 14 kV. Furthermore, the decrease in transmittance values is due to the higher discharge voltage applied during film growth. The band gap was slightly modified by the change in plasma condition, with values of 3.15 eV at 13 kV and 3.0 eV at 14 kV. Results showed that the extinction coefficient and refractive index of the prepared samples decrease with increasing discharge voltage. TiO_2:Sn thin films showed voltage-dependent sensing; 12 kV films had higher resistance and better NO_2 adsorption than 14 kV films. TiO_2:Sn thin films show decreasing NO_2 sensitivity with higher discharge voltage, due to increased charge carrier recombination suppressing the response.

1 INTRODUCTION

In recent years, researchers have been interested in materials for various applications, one of which is titanium oxide (TiO_2). A variety of applications for this material could include catalysis, solar cells, and photocatalysis [1]-[6]. TiO2 became an essential material for industrial usage due to its appropriate properties, such as a wide bandgap, with a value of 3.03 eV for rutile and 3.18 eV for anatase. Furthermore, the absorbance of ultraviolet wavelength is 5% of the sunlight. Scientists used different ways to deposit TiO2 particles, focusing on thin film form [7], [8]. The preparation of TiO2 thin films for use as photocatalysts became a viable option because the catalyst layer could be linked to an external power source. This connection reduces the recombination between holes and electrons generated by ultraviolet light, enhancing the effectiveness of the catalyst. The formation of the produced phase depends on the material composition, preparation technique, and annealing temperature. In general produce thin film, a variety of coating methods would be used, including thermal [9], anodic [10], sol–gel method [11], ion beam [12], CVD [13], Plasma spray [14], SPT [15], PLD [16], [17], PECVD [18], and RF sputtering method [19], [20]. In this study, the discharge voltage variation during the plasma jet technique preparation of TiO_2:Sn thin films is examined, along with the investigation of their physical, structural, and optical properties.

2 EXPERIMENTAL

Thin films of TiO_2:Sn were obtained by the atmospheric pressure plasma jet method. In this work, argon was used as the working gas at a flow rate of 0.5 L/min, and discharge voltages of 12, 13, and 14 kV were applied between the electrodes to investigate

the effect of discharge voltage on the properties of the films. The plasma nozzle was located 2 cm from the surface of 10 mL of DI water. A titanium sheet (99.99%) was cut and used as a target inside the reactor. In deionized water, the titanium surface was slowly oxidized by plasma plume to obtain titanium oxide (TiO_2) nanoparticles. These nanoparticles were then incorporated into a precursor solution of tin ($SnCl_2$) that was introduced to the plasma environment to create core-shell TiO_2:Sn nanoparticles. During the process, the presence of reactive plasma species and solution allowed the deposition of tin in a titanium oxide matrix. Considering the influence of discharge voltage, the synthesis was conducted under the same conditions applied to each voltage level. The color changes of the resulting colloidal suspensions verified the formation of nanoparticles. After synthesis, the drop-casting technique was used to deposit the as-obtained TiO_2:Sn nanoparticles on pre-cleaned glass substrates. The deposited droplets were allowed to dry at room temperature, forming thin films that were visually observed on the substrate's surface. As-deposited films were then transferred into a laboratory furnace at 150 °C for 30 minutes to promote densification, surface uniformity, and adhesion. After XRD, AFM, SEM, and UV–Vis characterization, the thin films of TiO_2:Sn were annealed, resulting in a compact and homogeneous appearance, with better adhesion due to this annealing process. Gas sensitivity measurements are typically conducted using a cylindrical testing chamber with a radius of 9 cm and a height of 17 cm.

3 RESULTS AND DISCUSSIONS

The structural properties of the synthesized films, as shown in Figure 1, were investigated using X-ray diffraction (XRD) analysis. The diffraction pattern reveals characteristic peaks located at 25.26°, 37.60°, 48.23°, and 55.04°, which are indexed to the (101), (004), (200), and (211) crystallographic planes, respectively, in good agreement with ICDD card No. 21-1272. The presence of these well-defined reflections confirms the polycrystalline nature of the films, with a dominant preferred orientation along the (101) plane. This preferential growth suggests that atomic arrangement along this direction is energetically more favorable, likely due to lower surface energy and denser atomic packing [21], [22].

The crystallite size (D) was estimated using the Scherrer relation [23], [24]. The calculated values, obtained from the main diffraction peaks, range from 16.93 nm to 19.39 nm, with an average value of approximately 16.93 nm. The relatively small variation in crystallite size indicates a fairly uniform grain distribution, suggesting stable and controlled nucleation and growth conditions during film formation, which promote consistent microstructural evolution across the samples [25], [26].

The dislocation density (δ) was evaluated using the standard relation reported in [27], [28]. The obtained value for the film prepared at 12 kV is 34.82 × 10^{14} m^{-2}, and it shows a decreasing trend with increasing discharge voltage. This reduction in dislocation density reflects improved crystalline quality and enhanced structural ordering at higher voltages. The increase in deposition energy promotes better atomic rearrangement, resulting in more uniform grain growth and a lower concentration of lattice defects within the films [29], [30].

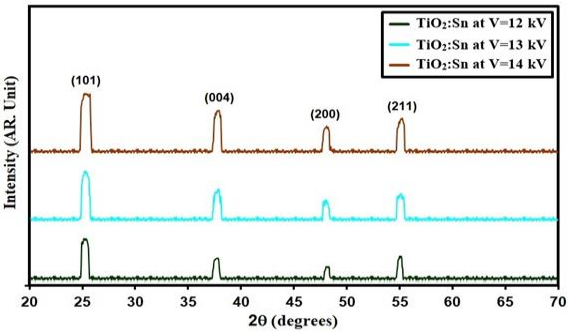

Figure 1: XRD styles of TiO_2:Sn films.

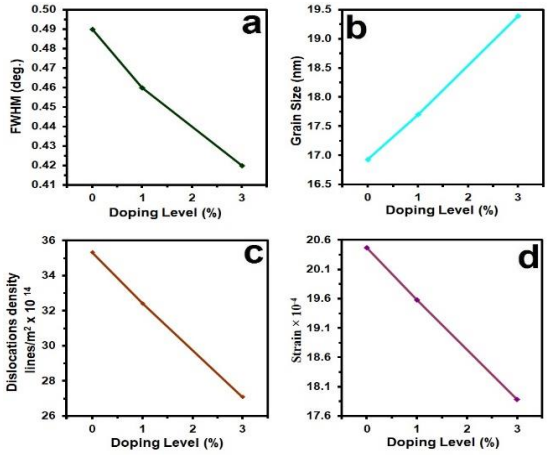

Figure 2: FWHM (a) *D* (b) δ (c) ε (d) of TiO_2:Sn films.

The lattice strain (ε) was calculated using the method described in [31], [32]. The results show that strain decreases from 20.47 × 10^{-4} to 17.88 × 10^{-4} as the discharge voltage increases, as illustrated in

Figure 2. This decline indicates a gradual relaxation of internal stresses and improved structural stability with higher deposition energy, which contributes to enhanced crystallinity of the films [33], [34]. The complete set of structural parameters (Sp) is summarized in Table 1 and illustrated in Figure 2.

The surface morphology of the TiO_2:Sn thin films was analyzed using Atomic Force Microscopy (AFM), as presented in Figure 3. The topographical images (a3, b3, and c3) demonstrate the influence of discharge voltage on surface features. The analysis shows that the average particle size (P_{av}) increases from 52.64 nm to 81.79 nm, while the root mean square (RMS) roughness increases from 3.31 nm to 5.98 nm for films deposited at 12 kV, 13 kV, and 14 kV, respectively. Similarly, the overall surface roughness increases from 5.13 nm to 9.73 nm with increasing discharge voltage. This behavior can be attributed to the higher kinetic energy available during deposition at elevated voltages, which enhances nucleation dynamics and promotes grain growth, leading to larger particles and a rougher surface morphology [35], [36]. The detailed AFM parameters (P_aFM) are provided in Table 2.

Table 1: D, optical bandgap, and S_p of grown films.

Specimen	2 q (°)	(hkl) Plane	FWHM (°)		E_g (eV)	*D* (nm)	δ (× 10^{14}) (lines/m^2)	E (× 10^{-4})
TiO_2:Sn at V=12 kV	25.26	101	0.49		3.15	16.93	34.82	20.47
TiO_2:Sn at V=13 kV	25.23	101	0.46		3.09	17.70	31.91	19.58
TiO_2:Sn at V=14 kV	25.21	101	0.42		3.00	19.39	26.59	17.88

Table 2: P_{AFM} of TiO_2:Sn films.

Samples	P_{av} (nm)	R_a (nm)	R. M. S. (nm)
TiO_2:Sn at V=12kV	52.64	5.13	3.31
TiO_2:Sn at V=13kV	71.73	8.95	4.00
TiO_2:Sn at V=14kV	81.79	9.73	5.98

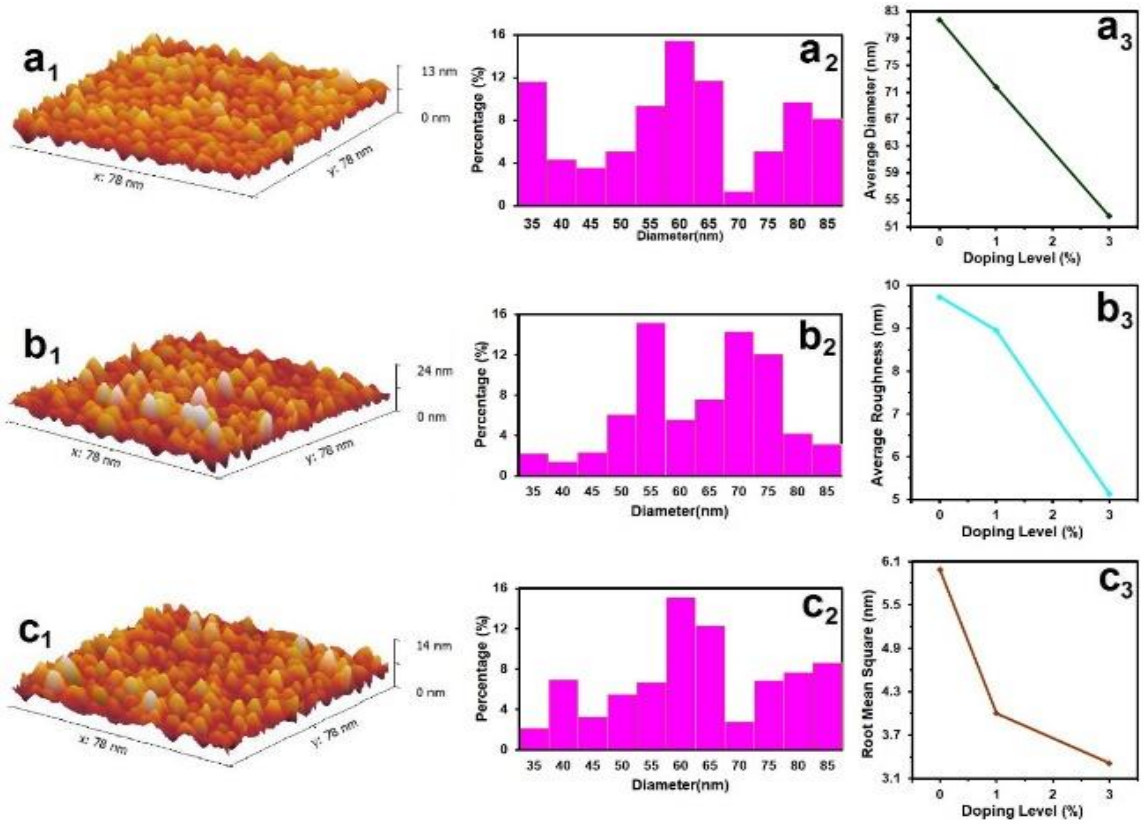

Figure 3: AFM images, granularly distributed P_{AFM} of TiO_2:Sn films.

Figure 4 shows the optical transmittance spectra of TiO_2:Sn thin films prepared at different discharge voltages. A gradual decrease in transmittance is observed, dropping from about 80% at 12 kV to approximately 75% at 14 kV. This reduction can be explained by structural modifications induced by increasing discharge voltage, particularly grain growth and improved crystallinity, which enhance scattering and absorption of incident photons within the film, thereby lowering the transmitted light intensity [23], [24].

The absorption coefficient (α) was calculated using the standard relation reported in [37], [38], where film thickness is taken into account. The variation of α with discharge voltage is presented in Figure 5. The results indicate that the absorption coefficient increases with increasing discharge voltage. This trend suggests stronger light–matter interaction at higher voltages, which can be attributed to improved crystallinity and increased surface roughness, both of which enhance photon absorption within the material [39], [40].

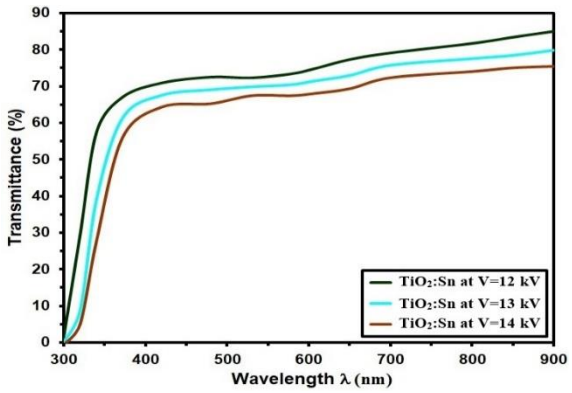

Figure 4: T of TiO_2:Sn films.

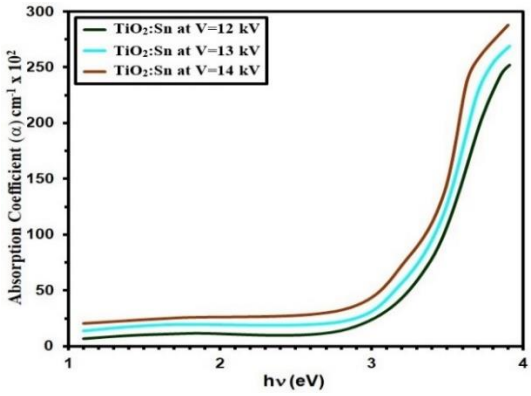

Figure 5: α of TiO_2:Sn films.

The optical bandgap (Eg) of the TiO_2:Sn thin films was determined using the Tauc relation for direct allowed transitions [41], [42]. The corresponding analysis is presented in Figure 6. The results show a clear dependence of the optical bandgap on discharge voltage, reflecting changes in the electronic structure of the films induced by deposition conditions. Increased voltage leads to structural and optical modifications that influence the energy required for electronic transitions, thereby affecting Eg.

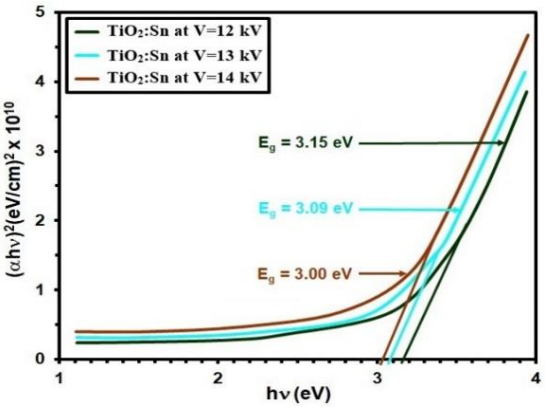

Figure 6: $(\alpha h\nu)^2$ of TiO_2:Sn films.

Figure 7 illustrates the spectral dependence of the extinction coefficient (k) as a function of wavelength (λ), evaluated using the relation given in [45], [46]. In this expression, λ denotes the incident light wavelength. The results indicate that the extinction coefficient decreases with increasing discharge voltage. This behavior can be attributed to structural improvements in the films, particularly enhanced crystallinity and reduced defect density at higher voltages, which collectively reduce light scattering and absorption losses within the material [47], [48].
The refractive index (n) was determined using the optical relation reported in [49], [50], where reflectance (R) and extinction coefficient (k) are taken into account. The variation of n with wavelength is shown in Figure 8 for all prepared films. The results reveal that the refractive index decreases as the discharge voltage increases. This trend can be explained by improved film densification and reduced defect concentration at higher deposition energies, which lead to a decrease in material polarizability and, consequently, a lower refractive index [51], [52].

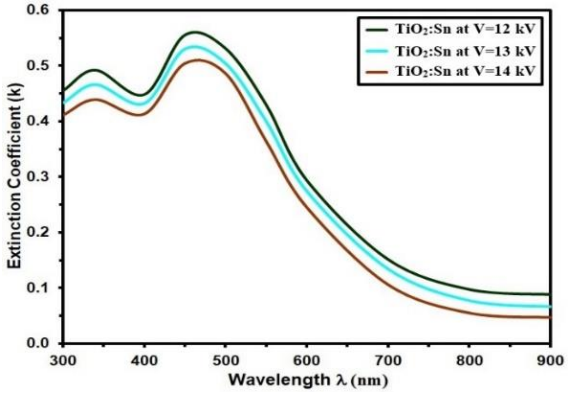

Figure 7: *K* of TiO_2:Sn films.

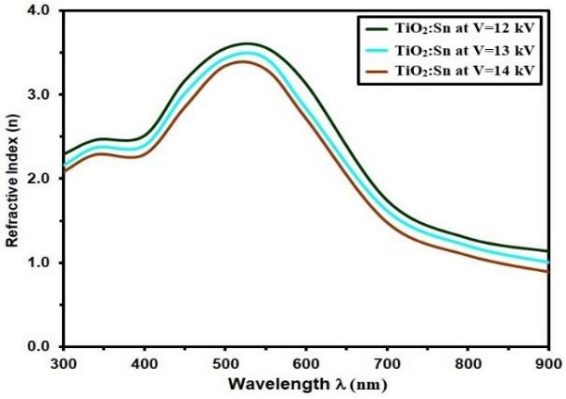

Figure 8: n of the TiO_2:Sn films.

The gas sensing characteristics of TiO_2:Sn thin films deposited at different discharge voltages were investigated at an operating temperature of 150 °C. As shown in Figure 9, the resistance variation was recorded during exposure to 270 ppm NO_2 gas. The film prepared at 12 kV exhibits the highest resistance response, indicating stronger adsorption of NO_2 molecules on the surface and more pronounced charge transfer interactions with the semiconductor. This enhanced interaction contributes to improved sensing activity and greater responsiveness of the material [53], [54]. In contrast, the film deposited at 14 kV shows the lowest resistance response, which may be related to changes in its electronic structure and reduced surface reactivity induced by higher discharge energy [55], [56].

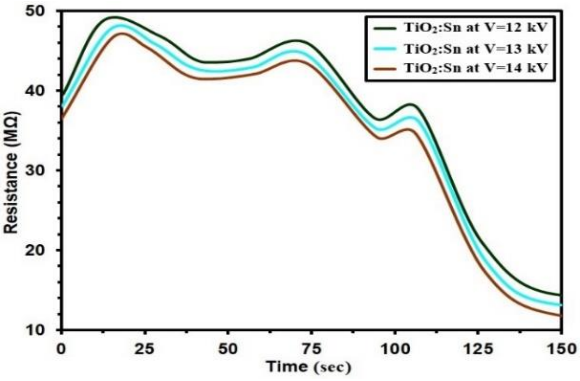

Figure 9: Resistance variation over time of TiO_2:Sn thin films synthesized at different discharge voltages during gas sensing operation.

The gas sensor sensitivity was calculated using the standard relation given in [57], [58], where the response is defined based on the relative change in resistance. In this expression, R_g represents the baseline resistance in air and R_a is the resistance in the presence of NO_2 gas. The sensitivity behavior of TiO_2:Sn thin films at different discharge voltages under various NO_2 concentrations is presented in Figure 10. The results clearly show that sensitivity decreases with increasing discharge voltage [59], [60]. Quantitatively, the sensitivity drops from 32.98% to 6.96% at 90 ppm, from 34.05% to 7.76% at 180 ppm, and from 35.25% to 18.77% at 270 ppm when comparing films prepared at 12 kV with those at higher discharge voltages [61], [62]. This decline in sensitivity is mainly attributed to enhanced charge carrier recombination at higher voltages, which reduces the effective separation of charge carriers and weakens the overall sensor response to NO_2 gas [63].

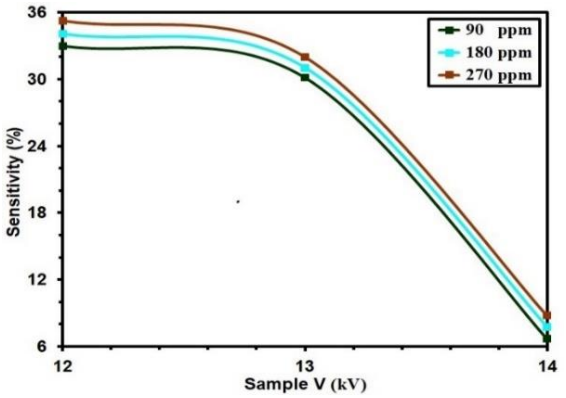

Figure 10: The sensitivity of TiO_2:Sn thin films synthesized at different discharge voltages.

4 CONCLUSIONS

The plasma jet technique was utilized to prepare undoped TiO_2:Sn thin films. It was found that the thickness of the films is 330 ± 20 nm at a temperature of 400°C. The XRD results showed that the dominant peak at the (101) plane for all films prepared at different discharge voltages exhibited a cubic polycrystalline structure. AFM analysis revealed an average grain size between 81.79 nm and 53.64 nm, with an average roughness of (9.73 – 5.13) nm. In addition, the root mean square roughness (R_{rms}) increased with increasing discharge voltage, with values of 6.36 nm for the film prepared at 12 kV and 7.61 nm for the film prepared at 14 kV. The transmittance of TiO_2:Sn films decreased from 80% to 75% as the discharge voltage increased. Meanwhile, the absorption coefficient increased with increasing voltage in TiO_2:Sn thin films. The optical energy gap was decreased from 3.15 eV for the film prepared at 12 kV to 3.00 eV for the film prepared at higher voltages. Moreover, both the extinction coefficient and refractive index decreased with increasing discharge voltage in TiO_2:Sn thin film. CuO film at 12 kV shows higher resistance and better NO_2 adsorption, while TiO_2 at 14 kV exhibits lower resistance due to electronic changes. Increasing discharge voltage in TiO_2:Sn films reduces NO_2 sensitivity due to enhanced charge carrier recombination, limiting effective charge separation.

ACKNOWLEDGMENTS

The support for this paper came from Mustansiriyah University (www.uomustansiriyah.edu.iq), which the submitters wish to appreciate.

REFERENCES

[1] D.G. Cahill and T.H. Allen, “Thermal conductivity of sputtered and evaporated SiO2 and TiO2 optical coatings,” Appl. Phys. Lett., vol. 65, p. 309, 1994, [Online]. Available: https://doi.org/10.1063/1.112355.

[2] S. Ben Amor, G. Baud, J.P. Besse and M. Jacquet, “Structural and optical properties of sputtered titanium films,” Mater. Sci. Eng. B, vol. 47, pp. 110-118, 1997.

[3] P.S. Shinde, H.P. Deshmukh, S.H. Mujawar, A.I. Inamdar and P.S. Patil, “Spray deposited titanium oxide thin films as passive counter electrodes,” Electrochim. Acta, vol. 52, pp. 3114-3120, 2007.

[4] B. O’Regan and M. Grätzel, “A low-cost, high-efficiency solar cell based on dye-sensitized colloidal TiO2 films,” Nature, vol. 353, pp. 737-740, 1991, [Online]. Available: https://doi.org/10.1038/353737a0.

[5] K.S. Kim and M.A. Barteau, “Structure and composition requirements for deoxygenation, dehydration, and ketonization reactions of carboxylic acids on TiO2 (001) single crystal surfaces,” J. Catal., vol. 125, pp. 353-375, 1990.

[6] P. Babelon, A.S. Dequiedt, H. Mostesa-Sba, S. Bourgeois, P. Sibillot and M. Sacilotti, “SEM and XPS studies of titanium dioxide thin films grown by MOCVD,” Thin Solid Films, vol. 322, pp. 63-67, 1998.

[7] R.W. Matthews, “Photooxidation of organic impurities in water using thin films of titanium dioxide,” J. Phys. Chem., vol. 91, pp. 3328-3333, 1987, [Online]. Available: https://doi.org/10.1021/j100296a044.

[8] A. Fujishima, T.N. Rao and D.A. Tryk, “Titanium dioxide photocatalysis,” J. Photochem. Photobiol. C, vol. 1, pp. 1-21, 2000.

[9] B.M. Henry, “Method of depositing titanium dioxide (rutile) as a gate dielectric for MIS device fabrication,” US Patent 4,200,474, 1978.

[10] M.R. Kozlowski, P.S. Tyler, W.H. Smyrl and R.T. Atanasoski, “Anodic TiO2 thin films: photoelectrochemical, electrochemical, and structural study of heat-treated and RuO2-modified films,” J. Electrochem. Soc., vol. 136, pp. 442-450, 1989.

[11] J.Y. Kim, D.W. Kim, H.S. Jung and K.S. Hong, “Influence of anatase-rutile phase transformation on dielectric properties of sol-gel derived TiO2 thin films,” Jpn. J. Appl. Phys., vol. 44, pp. 6148-6151, 2005.

[12] C. Yang, H. Fan, Y. Xi, J. Chen and Z. Li, “Effects of depositing temperatures on structure and optical properties of TiO2 film deposited by ion beam assisted electron beam evaporation,” Appl. Surf. Sci., vol. 254, pp. 2685-2689, 2008.

[13] V.G. Besserguenev, R.J.F. Pereira, M.C. Mateus, I.V. Khmelinskii, R.C. Nicula and E. Burkel, “TiO2 thin film synthesis from complex precursors by CVD, its physical and photocatalytic properties,” Int. J. Photoenergy, vol. 5, pp. 99-105, 2003.

[14] M.A. Issa and K.A. Aadim, “Optical and structural characterization of ZnO:NiO nanocomposite prepared by pulsed laser deposition method,” J. Opt., vol. 54, pp. 2357-2362, 2025.

[15] H.P. Deshmukh, P.S. Shinde and P.S. Patil, “Structural, optical and electrical characterization of spray-deposited TiO2 thin films,” Mater. Sci. Eng. B, vol. 130, pp. 220-227, 2006.

[16] M.A. Issa and K.A. Aadim, “Study the structural and optical properties of zinc oxide prepared by pulse laser deposition,” J. Opt., 2024.

[17] M.A. Issa and K.A. Aadim, “Influence of laser energy on structural and optical properties of ZnO(x):NiO(1-x) films prepared by pulse laser deposition,” J. Opt., 2024.

[18] W. Yang and C.A. Wolden, “Plasma-enhanced chemical vapor deposition of TiO2 thin films for dielectric applications,” Thin Solid Films, vol. 515, pp. 1708-1713, 2006.

[19] O. Banakh, P.E. Schmid, R. Sanjines and F. Levy, "Electrical and optical properties of TiOx thin films deposited by reactive magnetron sputtering," Surf. Coat. Technol., vol. 151-152, pp. 272-275, 2002.

[20] P.B. Nair, V.B. Justinvictor, G.P. Daniel, K. Joy and P.V. Thomas, "Influence of film thickness and annealing atmosphere on the structural, optical and luminescence properties of nanocrystalline TiO2 thin films prepared by RF magnetron sputtering," J. Mater. Sci.: Mater. Electron., vol. 24, pp. 2453-2460, 2013.

[21] M.M. Momenin and Y. Ghayeb, "Preparation of cobalt coated TiO2 and WO3-TiO2 nanotube films via photo-assisted deposition with enhanced photocatalytic activity under visible light illumination," Ceram. Int., vol. 42, pp. 7014-7022, 2016.

[22] J. Xu, S. Shi, L. Li, X. Zhang, Y. Wang, X. Chen, J. Wang, L. Lv, F. Zhang and W. Zhong, "Structural, optical, and ferromagnetic properties of Co-doped TiO2 films annealed in vacuum," J. Appl. Phys., vol. 107, p. 053910, 2010.

[23] R.R. Ahmed, T.H. Mubarak and I.H. Mohamed, "A study of structural and chemical properties of Ni1-xZnxFe2O4 ferrite powder prepared by co-precipitation method," Digest J. Nanomater. Biostruct., vol. 17, pp. 741-748, 2022.

[24] B.A. Bader, S.K. Muhammad, A.M. Jabbar, K.H. Abass, S.S. Chiad and N.F. Habubi, "Synthesis and characterization of indium-doped CdO nanostructured thin films: a study on optical, morphological, and structural properties," J. Nanostruct., vol. 10, pp. 744-750, 2020.

[25] N. Venkatachalam, M. Palanichamy, B. Arabindoo and V. Murugesan, "Enhanced photocatalytic degradation of 4-chlorophenol by Zr4+ doped nano TiO2," J. Mol. Catal. A Chem., vol. 266, pp. 158-165, 2007.

[26] K. Bouabid, A. Ihlal, Y. Amir, A. Sdaq, A. Assabbane, Y. Ait-Ichou, A. Outzourhit, E.L. Ameziane and G. Nouet, "Optical study of TiO2 thin films prepared by sol-gel," Ferroelectrics, vol. 372, pp. 69-75, 2008.

[27] R.S. Ali, N.A.H. Al Aaraji, E.H. Hadi, K.H. Abass, N.F. Habubi and S.S. Chiad, "Effect of lithium on structural and optical properties of nanostructured CuS thin films," J. Nanostruct., vol. 10, pp. 810-816, 2020.

[28] M. Hamadanian, A. Reisi-Vanani and A. Majedi, "Sol-gel preparation and characterization of Co/TiO2 nanoparticles: application to the degradation of methyl orange," J. Iran. Chem. Soc., vol. 7, pp. 52-58, 2010.

[29] H. Pulker, G. Paesold and E. Ritter, "Refractive indices of TiO2 films produced by reactive evaporation of various titanium-oxygen phases," Appl. Opt., vol. 15, pp. 2986-2991, 1976.

[30] H.Y. Ha, S.W. Nam, T.H. Lim, I.H. Oh and S.A. Hong, "Properties of the TiO2 membranes prepared by CVD of titanium tetraisopropoxide," J. Membr. Sci., vol. 111, pp. 81-92, 1996.

[31] H.S. Al-Rikabi, M.H. Al-Timimi and W.H. Albanda, "Morphological and optical properties of MgO1-xZnSx thin films," Digest J. Nanomater. Biostruct., vol. 17, pp. 889-897, 2022.

[32] A.J. Ghazai, O.M. Abdulmunem, K.Y. Qader, S.S. Chiad and N.F. Habubi, "Investigation of some physical properties of Mn doped ZnS nano thin films," AIP Conf. Proc., vol. 2213, p. 020101, 2020.

[33] P.J.L. Herve and L.K.J. Vandamme, "General relation between refractive index and energy gap in semiconductors," Infrared Phys. Technol., vol. 35, pp. 609-615, 1994.

[34] S. Douven, J.G. Mahy, C. Wolfs, C. Reyserhove, D. Poelman, F. Devred, E.M. Gaigneaux and S.D. Lambert, "Efficient N, Fe co-doped TiO2 active under cost-effective visible LED light: from powders to films," Catalysts, vol. 10, p. 547, 2020.

[35] S. Bhat, K.M. Sandeep, P. Kumar, S.M. Dharmaprakash and K. Byrappa, "Characterization of transparent semiconducting cobalt doped titanium dioxide thin films prepared by sol-gel process," J. Mater. Sci.: Mater. Electron., vol. 29, pp. 1098-1106, 2018.

[36] V.C. Ferreira, M.R. Nunes, A.J. Silvestre and O.C. Monteiro, "Synthesis and properties of Co-doped titanate nanotubes and their optical sensitization with methylene blue," Mater. Chem. Phys., vol. 142, pp. 355-362, 2013.

[37] S.S. Chiad, N.F. Habubi, W.H. Abass and M.H. Abdul-Allah, "Effect of thickness on the optical and dispersion parameters of Cd0.4Se0.6 thin films," J. Optoelectron. Adv. Mater., vol. 18, pp. 822-826, 2016.

[38] M.M. Khalaf, H.M.A. El-Lateef and H.M. Ali, "Optical and photocatalytic measurements of Co-TiO2 nanoparticle thin films," Plasmonics, vol. 13, pp. 1795-1802, 2018.

[39] J. Tian, H. Deng, L. Sun, H. Kong, P. Yang and J. Chu, "Effects of Co doping on structure and optical properties of TiO2 thin films prepared by sol-gel method," Thin Solid Films, vol. 520, pp. 5179-5183, 2012.

[40] C. Rath, P. Mohanty, V. Pandey and C. Mishra, "Oxygen vacancy induced structural phase transformation in TiO2 nanoparticles," J. Phys. D, vol. 42, p. 205101, 2009.

[41] Z. Tan, K. Sato and S. Ohara, "Synthesis of layered nanostructured TiO2 by hydrothermal method," Adv. Powder Technol., vol. 26, pp. 296-302, 2015.

[42] A. Ghazai, K. Qader, N.F. Habubi, S.S. Chiad and O. Abdulmunem, "Structural and optical performance of the doped ZnO nano-thin films by CSP," IOP Conf. Ser.: Mater. Sci. Eng., vol. 870, p. 012048, 2020.

[43] A. Boutlala, F. Bourfaa, M. Mahtili and A. Bouaballou, "Deposition of Co-doped TiO2 thin films by sol-gel method," IOP Conf. Ser.: Mater. Sci. Eng., vol. 108, p. 012048, 2016.

[44] A. Chanda, S.R. Joshi, V.R. Akshay, S. Varma, J. Singh, M. Vasundhara and P. Shukla, "Structural and optical properties of multilayered undoped and cobalt doped TiO2 thin films," Appl. Surf. Sci., vol. 536, p. 147830, 2021.

[45] J.C. González-Torres, L.A. Cipriano, E. Poulain, V. Domínguez-Soria, R. García-Cruz and O. Olvera-Neria, "Optical properties of anatase TiO2: synergy between transition metal doping and oxygen vacancies," J. Mol. Model., vol. 24, pp. 1-11, 2018.

[46] S. Ghasemi, S. Rahimnejad, S.S. Rahman, S. Rohani and M.R. Gholami, "Transition metal ions effect on the properties and photocatalytic activity of nanocrystalline TiO2 prepared in an ionic liquid," J. Hazard. Mater., vol. 172, pp. 1573-1578, 2009.

[47] O.A. El-Gammal, A.E. Alsayed Fouda and D. Mohamed Nabih, "Synthesis, spectral characterization, DFT and in vitro antibacterial activity of Zn(II), Cd(II) and Hg(II) complexes derived from a new thiosemicarbazid," Lett. Appl. NanoBioScience, vol. 8, pp. 715-722, 2019.

[48] F. Mostaghni and Y. Abed, "Structural determination of Co/TiO2 nanocomposite: XRD technique and simulation analysis," Mater. Sci.-Poland, vol. 34, pp. 534-539, 2016.

[49] E.H. Hadi, M.A. Abbsa, A.A. Khadayeir, Z.M. Abood, N.F. Habubi and S.S. Chiad, "Effects of Mn doping on the characterization of nanostructured TiO2 thin films deposited via chemical spray pyrolysis method," J. Phys.: Conf. Ser., vol. 1664, p. 012094, 2020.

[50] A.A. Kamil, N.A. Bakr, T.H. Mubaraka and J. Al-Zanqanawee, "Effect of Au and Ag nanoparticles addition on the morphological, structural and optical properties of ZnO thin films deposited by sol-gel method," J. Ovonic Res., vol. 18, pp. 431-442, 2022.

[51] Z. Ding, X. Hu, P.L. Yue, G.Q. Lu and P.F. Greenfield, "Synthesis of anatase TiO2 supported on porous solids by chemical vapor deposition," Catal. Today, vol. 68, p. 173, 2001.

[52] G. Pecchi, P. Reyes, P. Sanhueza and J. Villasenor, "Photocatalytic degradation of pentachlorophenol on TiO2 sol-gel catalysts," Chemosphere, vol. 43, p. 141, 2001.

[53] Z.G. Hu, W.W. Li, J.D. Wu, J. Sun, Q.W. Shu, X.X. Zhong, Z.Q. Zhu and J.H. Chu, "Optical properties of pulsed laser deposited rutile titanium dioxide films on quartz substrates determined by Raman scattering and transmittance spectra," Appl. Phys. Lett., vol. 93, p. 181910, 2008.

[54] A.E.D. Mahmoud, "Nanomaterials: green synthesis for water applications," in O. Kharissova, L. Martínez and B. Kharisov (eds), Handbook of Nanomaterials and Nanocomposites for Energy and Environmental Applications, pp. 1-21, Springer, Cham, 2020.

[55] M. Abushad, M. Arshad, S. Naseem, S. Husain and W. Khan, "Role of Cr doping in tuning the optical and dielectric properties of TiO2 nanostructures," Mater. Chem. Phys., vol. 256, p. 123641, 2020.

[56] O.M. Abdulmunem, A.M. Jabbar, S.K. Muhammad, M.O. Dawood, S.S. Chiad and N.F. Habubi, "Investigation of Co-doped Cu2O thin films on the structural, optical and morphology by SPT," J. Phys.: Conf. Ser., vol. 1660, p. 012048, 2020.

[57] W. Zhu, Y. Xu, H. Li, B. Dai, H. Xu, C. Wang, Y. Chao and H. Liu, "Photocatalytic oxidative desulfurization of dibenzothiophene catalyzed by amorphous TiO2 in ionic liquid," Korean J. Chem. Eng., vol. 31, pp. 211-217, 2014.

[58] M.L. Grilli, M. Yilmaz, S. Aydogan and B.B. Cirak, "Room temperature deposition of XRD-amorphous TiO2 thin films: investigation of device performance as a function of temperature," Ceram. Int., vol. 44, pp. 11582-11590, 2018.

[59] R. Renugadevi, T. Venkatachalam, R. Narayanasamy and S. Dinesh Kirupha, "Preparation of Co doped TiO2 nano thin films by sol-gel technique and photocatalytic studies of prepared films in tannery effluent," Optik, vol. 127, pp. 10127-10134, 2016.

[60] G. Sadanandam, K. Lalitha, V.D. Kumari, M.V. Shankar and M. Subrahmanyam, "Cobalt doped TiO2: a stable and efficient photocatalyst for continuous hydrogen production from glycerol: water mixtures under solar light irradiation," Int. J. Hydrogen Energy, vol. 38, pp. 9655-9664, 2013.

[61] N. Méndez-Lozano, M. Apátiga-Castro, A. Manzano-Ramírez, E.M. Rivera-Muñoz, R. Velázquez-Castillo, C. Alberto-González and M. Zamora-Antuñano, "Morphological study of TiO2 thin films doped with cobalt by metal organic chemical vapor deposition," Results Phys., vol. 16, p. 102891, 2020, [Online]. Available: https://doi.org/10.1016/j.rinp.2019.102891.

[62] B. Gong, X. Luo, N. Bao, J. Ding, S. Li and J. Yi, "XPS study of cobalt doped TiO2 films prepared by pulsed laser deposition," Surf. Interface Anal., vol. 46, pp. 1043-1046, 2014.

[63] A. Chanda, K. Rout, M. Vasundhara, S.R. Joshi and J. Singh, "Structural and magnetic study of undoped and cobalt doped TiO2 nanoparticles," RSC Adv., vol. 8, pp. 10939-10947, 2018.